https://doi.org/10.5194/egusphere-2025-4757
Preprint. Discussion started: 6 October 2025

Manuscript for

Divergent Drivers of Aerosol Acidity: Evidence for Shifting Regulatory Regimes in a Coastal Region

Authors: Jinghao Zhai[1,2], Yujie Zhang[1], Baohua Cai[1], Yaling Zeng[1,2], Jingyi Zhang[1], Jianhuai Ye[1,2], Chen Wang[1,2], Tzung-May Fu[1,2], Lei Zhu[1,2], Huizhong Shen[1,2], Xin Yang[1,2]*

[1]*Shenzhen Key Laboratory of Precision Measurement and Early Warning Technology for Urban Environmental Health Risks, School of Environmental Science and Engineering, Southern University of Science and Technology, Shenzhen 518055, China*

[2]*Guangdong Provincial Observation and Research Station for Coastal Atmosphere and Climate of the Greater Bay Area, Shenzhen 518055, China*

*To whom correspondence should be addressed.

Correspondence to: Xin Yang

Email: yangx@sustech.edu.cn

https://doi.org/10.5194/egusphere-2025-4757
Preprint. Discussion started: 6 October 2025

ABSTRACT: Aerosol acidity plays a crucial role in multiphase atmospheric chemistry, influencing aerosol composition, gas-particle partitioning, and the oxidative capacity of atmosphere. However, the mechanisms governing aerosol acidity in coastal area under extreme weather remains challenging due to its complexity of atmospheric transport. Here, we investigate aerosol pH in Shenzhen, a coastal megacity in China, by integrating field observations with multiphase buffer theory and ISORROPIA simulations. Our observations captured both a typhoon episode and typical non-typhoon periods with two contrasting regimes: during non-typhoon periods, aerosols were consistently buffered by the NH_4^+/NH_3 pair, with relative humidity serving as the primary driver of pH variability, enabling reliable predictions using multiphase buffer theory. In contrast, during a typhoon episode, sea salt derived nonvolatile cations emerged as the dominant drivers, violating the charge balance for NH_4^+/NH_3 buffering and leading to poor performance of buffer theory. Under these conditions, ISORROPIA simulations with constant aerosol water content reproduced the observed pH more reliably, highlighting a compositional rather than meteorological control. Our results provide the direct field-based evidence for regime shifts in aerosol acidity regulation in coastal area, and underscore the need for chemical transport models to account for composition-meteorology interactions to improve acidity predictions under extreme weather events.

Abstract Graphic

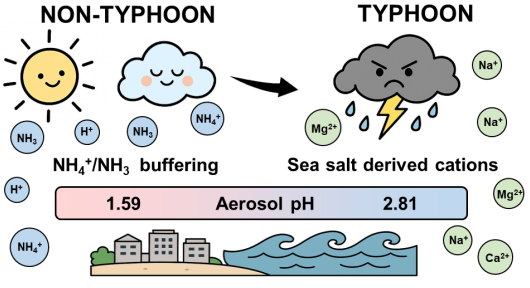

https://doi.org/10.5194/egusphere-2025-4757
Preprint. Discussion started: 6 October 2025

1 INTRODUCTION

Aerosol acidity is a key regulator in multiphase atmospheric chemistry. It governs the gas-particle partitioning of semi-volatile species (e.g., NH_3, HNO_3, HCl, and organic acids/bases) and dictates critical aqueous-phase processes, including SO_2 oxidation, secondary transformations of organic compounds, and the activation of trace metals (Tilgner et al., 2021;Pye et al., 2020;Cai et al., 2024;Surratt et al., 2007). Through these pathways, aerosol acidity exerts strong control over atmospheric oxidative capacity and pollutant lifetimes (Pye et al., 2020). On a large scale, aerosol acidity plays a pivotal role in determining particle composition, optical properties, and hygroscopicity, thereby influencing their radiative impacts and the ability to act as cloud condensation nuclei (Turnock et al., 2019;Karydis et al., 2021;Xu et al., 2020;Zhang et al., 2023). Moreover, aerosol acidity enhances particle toxicity by directly triggering respiratory inflammation, and affects the solubility of heavy metals, thereby regulating their bioavailability in terrestrial and marine ecosystems (Fang et al., 2017;Song et al., 2024;Amdur et al., 1978;Longo et al., 2016). Variations in aerosol acidity are not only fundamental to atmospheric chemistry processes but also directly influence regional air quality management (e.g., coordinated control of $PM_{2.5}$ and ozone), the global nitrogen and sulfur cycles, and climate feedback mechanisms. Thus, advancing the understanding of aerosol acidity has critical implications for public health and environmental policy.

Precise quantification of aerosol acidity remains an important yet challenging issue in atmospheric chemistry. Aerosol acidity is typically determined by aerosol pH. Traditional methods based on filter extraction and subsequent H^+ quantification are susceptible to substantial artifacts arising from sampling and dilution (Pathak et al., 2004;Hennigan et al., 2015). Recent techniques, such as Raman-based microdroplet pH detection (Cui et al., 2021), aerosol optical tweezers (Boyer et al., 2020), fluorescence probes (Li and Kuwata, 2023), and quantitative colorimetric imaging (Craig et al., 2018), have provided novel insights into particle-scale acidity, though their applicability to real-world aerosols remains limited, particularly for real-time dynamic monitoring of aerosol acidity. Indirect proxies including ion balance and gas-to-particle molar ratios, while

https://doi.org/10.5194/egusphere-2025-4757
Preprint. Discussion started: 6 October 2025

widely applied, suffer from systematic biases owing to neglected organic acid dissociation and semi-volatile partitioning (Metzger et al., 2006;Hennigan et al., 2015). Thermodynamic equilibrium models have emerged as the dominant framework for estimating aerosol pH values (Saxena et al., 1986;Jacobson et al., 1996;Pilinis and Seinfeld, 1987;Wexler and Seinfeld, 1991). Among them, the Extended Aerosol Inorganic Model (E-AIM) and ISORROPIA are widely employed (Wexler and Clegg, 2002;Nenes et al., 1998), with E-AIM regarded as the benchmark owing to its explicit treatment of ion activity coefficients (Clegg et al., 1992), while ISORROPIA is favored for its computational efficiency (Nenes et al., 1999). Comparative studies generally report consistent pH estimates from these two models, albeit with context-dependent deviations (Song et al., 2018;Hennigan et al., 2015;Battaglia et al., 2019). Substantial uncertainties persist in characterizing the spatiotemporal variability of aerosol acidity and its dynamic response to chemical composition and meteorological drivers. Research remains limited in coastal megacities and under extreme weather events such as typhoons, where intense atmospheric transport may substantially challenge the applicability of existing models and theories.

Aerosol acidity exhibits strong spatiotemporal variability, mainly arising from the combined influences of particle chemical composition and meteorological conditions (Zhou et al., 2022;Zhang et al., 2021;Ding et al., 2019;Wang et al., 2022;Tao and Murphy, 2019, 2021). In particular, water-soluble inorganic components exert significant control, with sulfate substantially enhancing aerosol acidity due to its low volatility, whereas nitrate, with its strong hygroscopicity, increases aerosol water content (AWC) under elevated relative humidity, thereby lowering acidity (Ding et al., 2019). Therefore, a lower nitrate-to-sulfate ratio generally leads to more acidic particles (Xie et al., 2020). Although the direct contribution of organics to aerosol pH is relatively minor (Guo et al., 2015), interactions between inorganic and organic components can alter acidity with pH increases of up to 0.7 units (Pye et al., 2018). Meteorological conditions exert a strong influence on aerosol acidity by altering both particle water content and gas-particle partitioning. Increased relative humidity facilitates hygroscopic growth and promotes aqueous-phase reactions, which typically dilute proton concentrations and thus mitigate acidity (Bian et al., 2014). In

https://doi.org/10.5194/egusphere-2025-4757
Preprint. Discussion started: 6 October 2025

contrast, higher temperatures shift the equilibrium of semi-volatile species such as ammonia toward the gas phase and enhance water vapor pressure, processes that together elevate proton loading and intensify aerosol acidity (Guo et al., 2018;Battaglia et al., 2017). The recently proposed multiphase buffer theory provides a new framework for understanding the long-term evolution of aerosol acidity by emphasizing the stabilizing role of conjugate acid-base pairs against external perturbations, thereby exerting critical control over sulfate formation pathways and other multiphase atmospheric processes (Zheng et al., 2020;Zheng et al., 2022;Chen et al., 2022;Gao et al., 2025), highlighting the complexity of aerosol acidity driving mechanisms. However, the relative importance of different buffering systems under complex meteorological conditions remains poorly constrained, and the potential dominance of nonvolatile cations (NVCs, e.g., Na^+, Ca^{2+}, Mg^{2+}, K^+) in coastal environments and during extreme weather events has not been systematically assessed with field evidence.

In this study, we investigated the buffering capacity and controlling factors of aerosol pH in Shenzhen, China, a subtropical coastal megacity frequently influenced by typhoons, by integrating field observations with multiphase buffer theory and ISORROPIA II simulations. Our field observations captured both a typhoon episode and typical non-typhoon periods, providing a natural contrast between distinct atmospheric regimes. By comparing the buffering capacity and key drivers of aerosol pH during typhoon and non-typhoon periods, we aim to shed light on the complex interactions between composition and meteorology that regulate aerosol acidity. Our results provide the field-based evidence the role of NVCs in modulating aerosol acidity under extreme weather conditions. These findings underscore the need to account for meteorology-composition interactions when applying multiphase buffer theory in coastal regions, and reveal important limitations of current models under episodic perturbations.

2 METHODS

2.1 Field Measurements. Field measurements were carried out at the Xichong site (22.48°N, 114.56°E) on the Dapeng Peninsula in Shenzhen, China, from August to September 2022. Detailed

https://doi.org/10.5194/egusphere-2025-4757
Preprint. Discussion started: 6 October 2025

information and site characteristics of Xichong have been described elsewhere(Zhai et al., 2025). Briefly, Xichong is located at the southeastern end of Shenzhen, a representative coastal megacity in southern China. During the field campaign, a Monitor for AeRosols and Gases in Ambient air (MARGA, Metrohm-Applikon, Netherlands) was utilized to measure online concentrations of major water-soluble gases (NH_3, SO_2, HNO_3, HCl) and aerosol ions (NH_4^+, Na^+, K^+, Ca^{2+}, Mg^{2+}, SO_4^{2-}, NO_3^-, Cl^-). Additional measurements at the site included $PM_{2.5}$ and O_3 mass concentrations, as well as key meteorological parameters (temperature, relative humidity, wind speed, and wind direction). In this study, the analysis period used was from 24 August to 11 September 2022, corresponding to the overlapping operational time of all deployed instruments, with all online data standardized to a temporal resolution of 1 h.

2.2 ISORROPIA Calculation. The pH is defined in terms of the activity of hydrogen ions (H^+) in aqueous solution, expressed on a molality basis as:

$$\mathrm{pH} = -\log_{10}[a(\mathrm{H}^+)] = -\log_{10}[\chi(\mathrm{H}^+) \cdot \gamma(\mathrm{H}^+)] \quad (1)$$

where $a(\mathrm{H}^+)$ is the activity of H^+, and $\chi(\mathrm{H}^+)$ and $\gamma(\mathrm{H}^+)$ denote the mole fraction and mole fraction-based activity coefficients of H^+ in aqueous solution, respectively. In this study, aerosol pH is calculated using ISORROPIA II (http://isorropia.epfl.ch), which provides direct predictions of ionic activity, gas partial pressure, and the phase volumes of solids and liquids. Here, the model considers the Na^+–NH_4^+–K^+–Ca^{2+}–Mg^{2+}–Cl^-–NO_3^-–SO_4^{2-} system and is run in "forward mode" under the "metastable" phase state, which avoids salt crystallization and is more representative of ambient aerosol conditions under high humidity. The model is driven by measured concentrations of major aerosol ions and gases, along with observed meteorological parameters. Aerosol pH was then calculated from the ISORROPIA output as:

$$\mathrm{pH} = -\log_{10}[\mathrm{H}^+_{\mathrm{aq}}] = -\log_{10}[1000 \cdot \mathrm{H}^+_{\mathrm{air}}/\mathrm{AWC}] \quad (2)$$

where $\mathrm{H}^+_{\mathrm{aq}}$ is the equilibrium hydronium ion concentration in ambient aerosol liquid water (mol L^{-1}), $\mathrm{H}^+_{\mathrm{air}}$ is the equilibrium hydronium ion concentration per unit volume of air (μg m^{-3}), and

https://doi.org/10.5194/egusphere-2025-4757
Preprint. Discussion started: 6 October 2025

AWC is the aerosol water content (μg m^{-3}). The factor 1000 accounts for the unit conversion between μg m^{-3} of air and mol L^{-1} of aerosol liquid water.

2.3 Multiphase Buffer Theory. A buffer system is defined as a chemical system that exhibits resilience to pH perturbations upon the addition of a certain amount of acid or base. In homogeneous aqueous solutions, the conjugate acid-base pairs are confined to the liquid phase, and thus the solution pH is governed exclusively by acid dissociation equilibria. In multiphase systems, however, the volatile components of the conjugate pairs can reside in both the gas and liquid phases, whereby the pH is modulated by the coupled effects of gas-liquid partitioning and dissociation equilibria. The recently proposed multiphase buffer theory introduced an analytical framework for the buffer capacity β of aerosol systems(Zheng et al., 2020). Here, β is defined as the amount of acid ($d\mathrm{n_{acid}}$) required to reduce pH by $d\mathrm{pH}$ units, or the amount of base ($d\mathrm{n_{base}}$) required to raise pH by $d\mathrm{pH}$ units. It thus characterizes the instantaneous buffering capacity, relating infinitesimal changes in acid/base content to the corresponding change in pH. In this study, β (mol kg^{-1}) is expressed as:

$$\beta = -\frac{d\mathrm{n_{acid}}}{d\mathrm{pH}} = \frac{d\mathrm{n_{base}}}{d\mathrm{pH}} = 2.303\left\{\frac{K_\mathrm{w}}{[\mathrm{H^+}]} + [\mathrm{H^+}] + \sum_i \frac{K_{\mathrm{a,i}}^{*}\cdot[\mathrm{H^+}]}{(K_{\mathrm{a,i}}^{*}+[\mathrm{H^+}])^2}\cdot [X_\mathrm{i}]_{\mathrm{tot}}^{*}\right\} \quad (3\text{–}1)$$

where K_w is the water dissociation constant (mol^2 kg^{-2}), $K_{\mathrm{a,i}}^{*}$ represents the effective acid dissociation constant of buffering agent X_i in gas-liquid multiphase systems (mol kg^{-1}), and $[X_\mathrm{i}]_{\mathrm{tot}}^{*}$ is the total equivalent molality of X_i, accounting for both gaseous and aqueous phases (mol kg^{-1}).

The self-buffering capacity of water is an inherent property conferring resistance to pH changes. Here, it is defined as:

$$\beta_{\mathrm{water}} = 2.303\left\{\frac{K_\mathrm{w}}{[\mathrm{H^+}]} + [\mathrm{H^+}]\right\} \quad (3\text{–}2)$$

which becomes appreciable only under extreme acidic (pH < 2) or alkaline (pH > 12) conditions, but is negligible within the typical aerosol pH range. In contrast, conjugate acid-base pairs (e.g., NH_4^+/NH_3, HNO_3/NO_3^-, HSO_4^-/SO_4^{2-}) dominate buffering within this range, while minor organic

https://doi.org/10.5194/egusphere-2025-4757
Preprint. Discussion started: 6 October 2025

acids contribute little (Zheng et al., 2020). Similar to bulk aqueous systems, the effective buffer range ($pK_{a,i}^{*}$ ±1) corresponds to the pH interval over which these conjugate pairs exert substantial buffering effects.

Previous study (Zheng et al., 2020) further introduced the dimensionless gas-liquid partitioning constant (K_g) to represent the equivalent molality of gaseous species dissolved in the aqueous phase. This formulation enables explicit treatment of gas-particle equilibria for buffering agents such as NH_4^+/NH_3 and HNO_3/NO_3^-. Corrections for non-ideality due to elevated ionic strength can also be incorporated through activity coefficients. Despite simplifying assumptions, such as equilibrium thermodynamics and the neglect of organic contributions, multiphase buffer theory provides a powerful framework for quantifying aerosol buffering mechanisms.

For the buffering agent NH_4^+/NH_3,

$$NH_3 + H_2O \leftrightarrow NH_4^+ + OH^- \quad (4\text{–}1)$$

$$K_g = \frac{[NH_3(g)]}{[NH_3(aq)]} = \frac{\rho_w}{H_{NH_3} \cdot R \cdot T \cdot AWC} \quad (4\text{–}2)$$

$$K_{a,NH_3}{}^{*} = \frac{[H^+(aq)] \cdot ([NH_3(aq)] + [NH_3(g)])}{[NH_4^+(aq)]} = K_{a,NH_3} \cdot \left(1 + \frac{\rho_w}{H_{NH_3} \cdot R \cdot T \cdot AWC}\right) \quad (4\text{–}3)$$

And for the buffering agent HNO_3/NO_3^-,

$$HNO_3 \leftrightarrow H^+ + NO_3^- \quad (5\text{–}1)$$

$$K_g = \frac{[HNO_3(g)]}{[HNO_3(aq)]} = \frac{\rho_w}{H_{HNO_3} \cdot R \cdot T \cdot AWC} \quad (5\text{–}2)$$

$$K_{a,HNO_3}{}^{*} = \frac{[H^+(aq)] \cdot ([NO_3^-(aq)])}{[HNO_3(aq) + HNO_3(g)]} = K_{a,HNO_3} / \left(1 + \frac{\rho_w}{H_{HNO_3} \cdot R \cdot T \cdot AWC}\right) \quad (5\text{–}3)$$

where K_{a,NH_3} and K_{a,HNO_3} are the classical dissociation constants of NH_3 and HNO_3 (mol kg^{-1}), ρ_w is the density of liquid water (1×10^{12} μg m^{-3}), R is the universal gas constant (8.205×10^{-2} atm L mol^{-1} K^{-1}), T is the absolute temperature (K), AWC is the aerosol water content (μg m^{-3}), and H_{NH_3} and H_{HNO_3} are the Henry's law coefficients (mol kg^{-1} atm^{-1}).

https://doi.org/10.5194/egusphere-2025-4757
Preprint. Discussion started: 6 October 2025

For ambient aerosols, non-ideality due to elevated ionic strength should be considered, as it directly influences the calculation of the effective acid dissociation constant. Accounting for this through the inclusion of activity coefficients, the expression for the effective acid dissociation constant in a non-ideal multiphase system is given as:

$$K_{\mathrm{a,NH_3}}{}^{*,\mathrm{ni}} = K_{\mathrm{a,NH_3}} \cdot \left(1 + \frac{\rho_{\mathrm{w}}}{H_{\mathrm{NH_3}} \cdot R \cdot T \cdot \mathrm{AWC}}\right) \cdot \frac{\gamma_{\mathrm{NH_4^+}}}{\gamma_{\mathrm{H^+}}} \quad (6\text{–}1)$$

$$K_{\mathrm{a,HNO_3}}{}^{*,\mathrm{ni}} = K_{\mathrm{a,HNO_3}} / \left(1 + \frac{\rho_{\mathrm{w}}}{H_{\mathrm{HNO_3}} \cdot R \cdot T \cdot \mathrm{AWC}}\right) / (\gamma_{\mathrm{NO_3^-}} \cdot \gamma_{\mathrm{H}}^{+}) \quad (6\text{–}2)$$

Finally, the buffer capacities associated with the NH_4^+/NH_3 and HNO_3/NO_3^- conjugate pairs are expressed as:

$$\beta_{\mathrm{NH_3}} = 2.303 \frac{K_{\mathrm{a,NH_3}}{}^{*,\mathrm{ni}} \cdot [\mathrm{H^+}]}{(K_{\mathrm{a,NH_3}}{}^{*,\mathrm{ni}} + [\mathrm{H^+}])^2} \cdot [\mathrm{NH_3(g) + NH_3(aq) + NH_4^+(aq)}]_{\mathrm{tot}}{}^{*} \quad (7\text{–}1)$$

$$\beta_{\mathrm{HNO_3}} = 2.303 \frac{K_{\mathrm{a,HNO_3}}{}^{*,\mathrm{ni}} \cdot [\mathrm{H^+}]}{(K_{\mathrm{a,HNO_3}}{}^{*,\mathrm{ni}} + [\mathrm{H^+}])^2} \cdot [\mathrm{NH_3(g) + NH_3(aq) + NH_4^+(aq)}]_{\mathrm{tot}}{}^{*} \quad (7\text{–}2)$$

Multiphase buffer theory thus establishes a quantitative framework linking aerosol acidity to multiphase equilibria. Further details of the theoretical derivation are presented in the Supporting Information (SI, Text S1 and Table S1).

3 RESULTS AND DISCUSSION

3.1 Buffer Capacity for Aerosol Multiphase Systems. In this study, MARGA measurements were conducted from 24 August to 10 September 2022 at the Xichong site. Meteorological conditions, chemical compositions obtained from MARGA, and the aerosol water content and pH values simulated by ISORROPIA throughout the sampling period are presented in Figure 1. During the sampling period, Typhoon Ma-on (No. 2209) passed over the sampling site at 15:00 local time on August 24, 2022. Upon its arrival, wind speed at Xichong reached 16.5 m s^{-1}, the highest of the observation period. Concurrent decreases in $PM_{2.5}$, ozone, and total water-soluble ion mass concentrations were observed, accompanied by pronounced increases in the fractional contributions of chloride, sodium, and other NVCs (e.g., Ca^{2+}, Mg^{2+}, K^+) (Figure 1a–d). This

https://doi.org/10.5194/egusphere-2025-4757
Preprint. Discussion started: 6 October 2025

211 interval is hereafter referred to as the typhoon episode (blue shading in Figure 1), with all
212 remaining periods considered non-typhoon episodes. The ISORROPIA-simulated pH values
213 averaged 2.81 ± 0.54 during the typhoon episode and 1.59 ± 0.45 during non-typhoon periods
214 (Figure 1e).

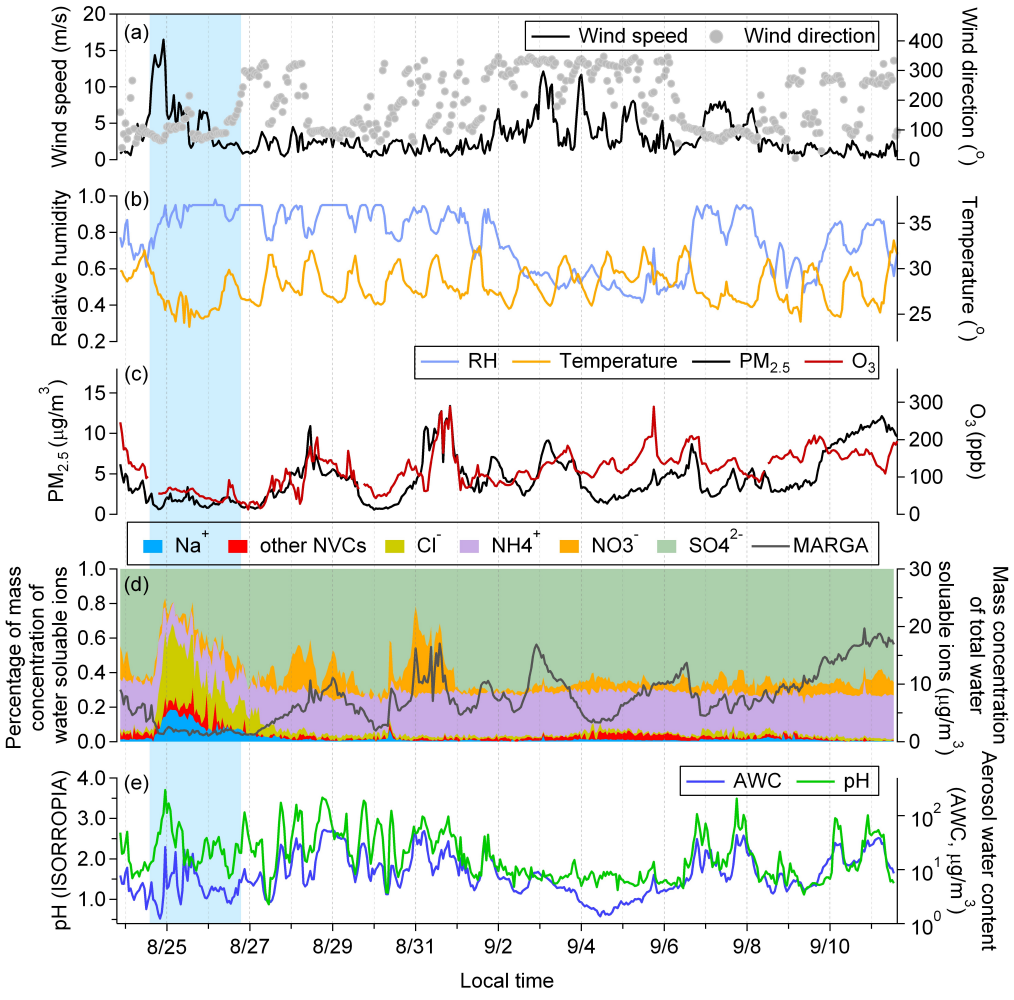

215

216 **Figure 1.** Time series of (a) wind direction and wind speed, (b) relative humidity (RH) and
217 temperature, (c) $PM_{2.5}$ and O_3 concentrations, (d) aerosol composition measured by MARGA, and
218 (e) aerosol pH and aerosol water content (AWC) simulated by ISORROPIA at the sampling site.

https://doi.org/10.5194/egusphere-2025-4757
Preprint. Discussion started: 6 October 2025

The gray line in panel (c) denotes the total concentration of water-soluble ions measured by MARGA. Other NVCs include Ca^{2+}, Mg^{2+}, and K^{+}. The blue shading indicates the typhoon period.

We applied the multiphase buffer theory to calculate the buffering capacities (β) of individual buffering agents (NH_4^+/NH_3, HNO_3/NO_3^-, and HSO_4^-/SO_4^{2-}) under both typhoon and non-typhoon scenarios. In both scenarios, the largest buffering capacity was associated with the NH_4^+/NH_3 pair, followed by HSO_4^-/SO_4^{2-} and HNO_3/NO_3^- (Figure 2). The peak buffer pH (defined as the pH corresponding to the highest local maximum of β) for the non-typhoon scenario was ~1.62 (Figure 2a), closely matching the ISORROPIA-modeled result (1.59 ± 0.45). In contrast, the peak buffer pH under typhoon scenario was ~1.70 (Figure 2b), showing a larger discrepancy from the ISORROPIA-simulated result (2.81 ± 0.54).

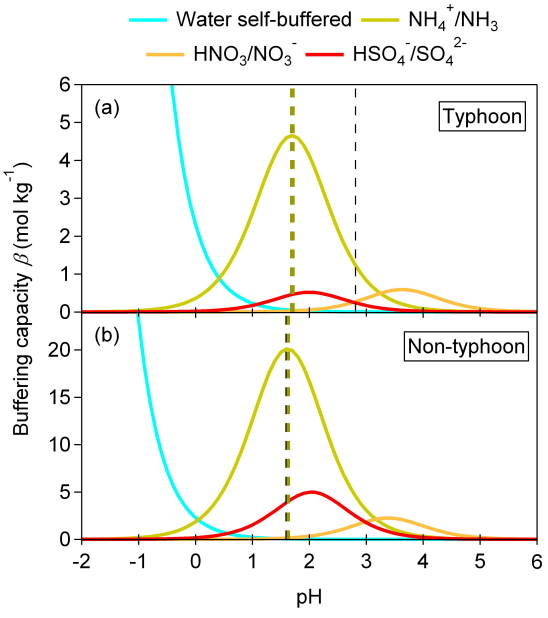

Figure 2. Buffering capacity (β) of the aerosol multiphase system for typhoon (a) and non-typhoon (b) scenarios. The olive dashed line indicates the pH corresponding to the highest local maximum of β, while the black dashed line represents the ISORROPIA-simulated pH.

https://doi.org/10.5194/egusphere-2025-4757
Preprint. Discussion started: 6 October 2025

The stronger role of NH_4^+/NH_3 under non-typhoon conditions reflects the abundance of ammonia in this coastal environment and its efficient partitioning, which provides stable buffering at acidic pH. However, for the typhoon scenario, the multiphase buffer theory appears to be less applicable. It should also be noted that multiphase buffer theory assumes instantaneous thermodynamic equilibrium and primarily considers inorganic conjugate acid-base pairs, while the potential contributions of organic species and kinetic effects are neglected. Such simplifications may further contribute to discrepancies under dynamic conditions.

3.2 Contribution of Individual Drivers. We further quantified the changes in aerosol pH (ΔpH) between typhoon and non-typhoon scenarios attributable to individual drivers (Figure 3), including anion-normalized nonvolatile cations (NVCs) and total ammonia (TNH_3), the fraction of total nitric acid ($THNO_3$) in anions, relative humidity (RH), and temperature (T). It should be noted that the perturbation constraints imposed on each driver differ both in magnitude and physical meaning (i.e., x-axis criteria in Figure 3, see Text S2 in SI). As a result, the ΔpH contributions of different drivers within the same scenario are not strictly comparable. Figure 3c presents the ΔpH contributions using absolute bar charts, which highlight their absolute magnitudes rather than relative shares. In contrast, the ΔpH contributions of a given driver between the typhoon and non-typhoon scenarios are derived under the same constraint framework and can therefore be meaningfully compared. In Figure 3, the blue and black dashed lines represent the corresponding values for typhoon and non-typhoon scenarios, respectively. For each driver, the ΔpH values correspond to the differences between the two scenarios used as constraints. The constraint ranges were selected to reflect the observed variability during the campaign, thereby ensuring that the perturbations remained within realistic atmospheric conditions.

The results indicate that RH, TNH_3, and temperature contributed substantially more to ΔpH in the non-typhoon scenario than in the typhoon scenario, with 0.75 vs. 0.26 units for RH, 0.36 vs. 0.16 units for TNH_3, and 0.15 vs. 0.01 units for temperature, respectively. Notably, NVCs was the only driver exhibiting a larger contribution to ΔpH in the typhoon scenario than in the non-typhoon scenario (0.27 vs. 0.09 units). In other words, the contribution of chemical components,

https://doi.org/10.5194/egusphere-2025-4757
Preprint. Discussion started: 6 October 2025

particularly NVCs, to ΔpH was more pronounced in the typhoon scenario, which partly explains the discrepancy between the pH predicted by the multiphase buffer theory and that calculated by ISORROPIA. This shift highlights a transition from meteorologically driven controls (RH and temperature) under non-typhoon conditions to compositionally driven controls dominated by sea-salt derived cations during the typhoon.

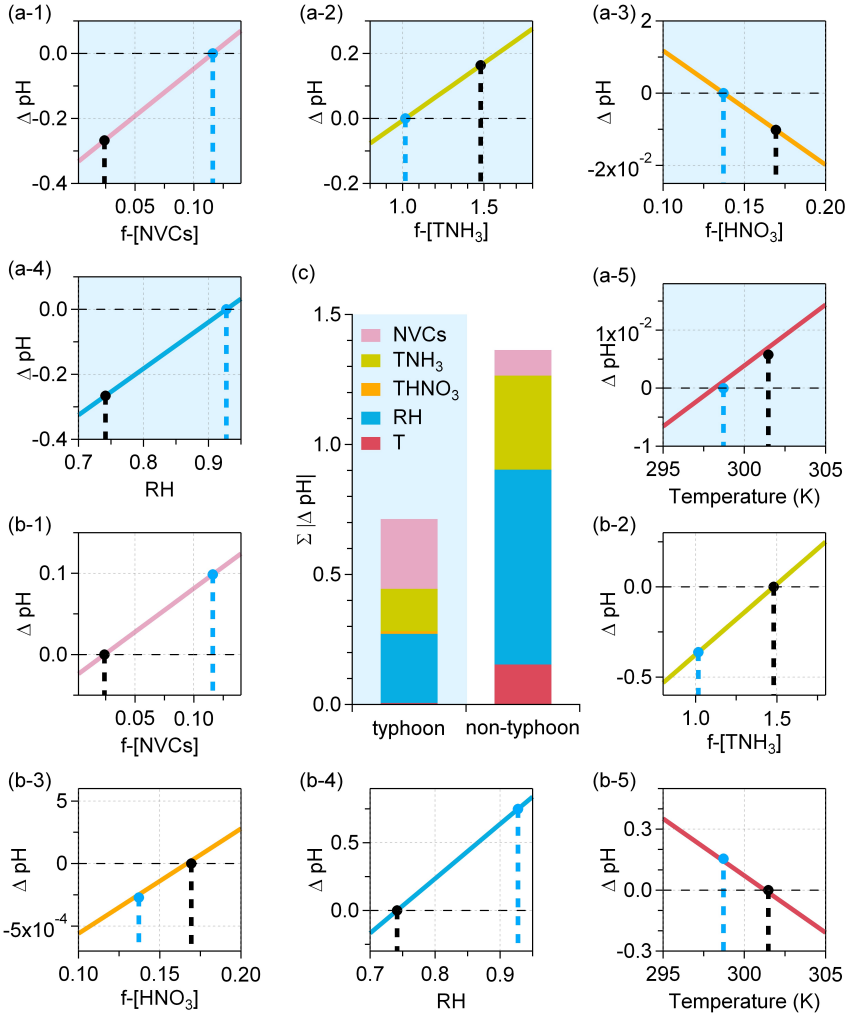

https://doi.org/10.5194/egusphere-2025-4757
Preprint. Discussion started: 6 October 2025

Figure 3. Aerosol pH differences (ΔpH) between typhoon (a1–5) and non-typhoon (b1–5) scenarios, attributed to anion-normalized non-volatile cations (NVCs) and total [NH_3] (TNH_3), the fraction of total [HNO_3] ($THNO_3$) in anions, relative humidity (RH), and temperature (T). The light blue background indicates simulations using typhoon conditions as inputs (a1–5), whereas the white background denotes simulations with non-typhoon conditions (b1–5). Panel (c) summarizes the total absolute ΔpH (Σ|ΔpH|) of different drivers in both scenarios. The blue and black dashed lines represent the corresponding values for typhoon and non-typhoon scenarios, respectively

Previous studies in inland regions (Zheng et al., 2020), such as the North China Plain and the southeastern United States, have emphasized ammonia availability and aerosol water as the primary determinants of aerosol acidity, whereas our results underscore the unique role of NVCs in coastal megacities under extreme weather influence. For NH_4^+/NH_3 to serve as the dominant buffering pair, two conditions must be satisfied (Zheng et al., 2020): (1) the equivalent charge of total cations exceeds that of total anions, and (2) the equivalent charge of NVCs is smaller than that of nonvolatile anions. In the typhoon scenario, however, the equivalent charge of NVCs exceeded that of nonvolatile anions, thereby violating the conditions required for NH_4^+/NH_3 to serve as the dominant buffering pair. This explains why the multiphase buffer theory fails to reliably predict aerosol pH under typhoon conditions. The enhanced influence of NVCs can be attributed to the substantial influx of sea-salt particles transported by strong winds and the altered trajectories of air masses during the typhoon. These inputs directly neutralize acidic species and disrupt the conventional NH_4^+/NH_3 buffering system, a process far less pronounced in inland settings.

We compared the ISORROPIA-simulated pH with that predicted by the multiphase buffer theory and with the ISORROPIA-simulated pH under a constant-AWC assumption, for typhoon and non-typhoon scenarios, respectively (Figure 4). The constant-AWC experiment was designed to isolate the role of chemical composition from that of aerosol water content, thereby allowing us to directly assess whether pH variability can be reproduced without explicitly accounting for

https://doi.org/10.5194/egusphere-2025-4757
Preprint. Discussion started: 6 October 2025

dynamic changes in AWC. The results show that under the non-typhoon scenario, ISORROPIA-simulated pH gives a stronger correlation with the multiphase buffer theory ($R^2 = 0.69$) than with the constant-AWC simulation ($R^2 = 0.30$). In contrast, under the typhoon scenario, ISORROPIA-simulated pH correlates well with constant-AWC ($R^2 = 0.73$), but poorly with the multiphase buffer theory ($R^2 = 0.21$). These findings indicate that in regimes or scenarios buffered by the NH_4^+/NH_3 pair, such as non-typhoon conditions in Shenzhen, variations in AWC alone can provide a reliable prediction of aerosol pH, even without explicitly accounting for the temporal and spatial variability in particle chemical composition. The buffering effect of ammonia suppresses the influence of compositional differences, making aerosol water content the primary determinant of aerosol pH. However, in environments that are not buffered by NH_4^+/NH_3, the influence of AWC on pH becomes weaker, and reliable predictions require explicit consideration of chemical composition within a constant-AWC framework.

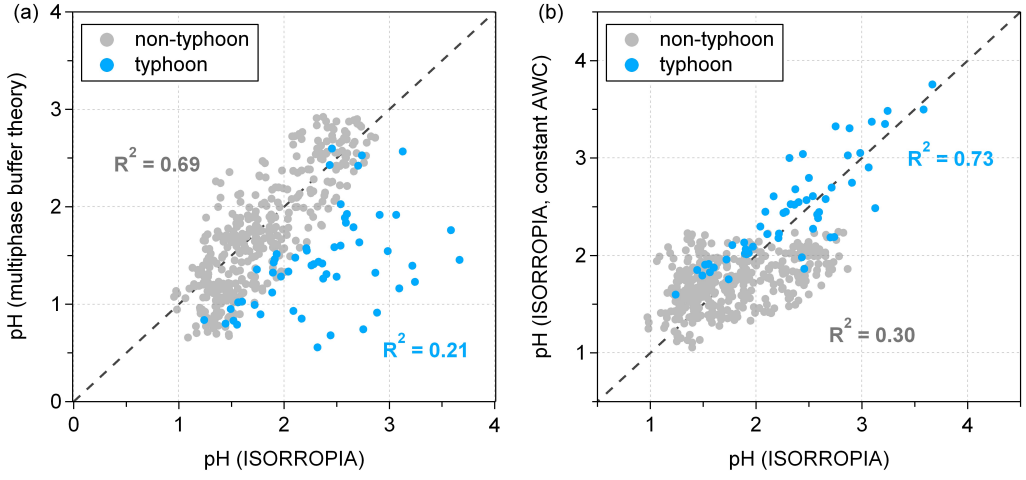

Figure 4. Correlations between aerosol pH simulated based on ISORROPIA and pH predicted by (a) the multiphase buffer theory, and (b) ISORROPIA under a constant aerosol water content (AWC) assumption with varying chemical compositions. Blue and gray dots represent typhoon and non-typhoon scenarios, respectively. The black dashed line indicates the 1:1 reference.

https://doi.org/10.5194/egusphere-2025-4757
Preprint. Discussion started: 6 October 2025

These results suggest that chemical composition plays a more critical role in determining pH under typhoon scenarios, whereas during non-typhoon periods, aerosol water content influenced by RH and temperature exerts a stronger impact on pH. While the multiphase buffer theory is robust under ammonia-buffered regimes, its applicability becomes limited in environments dominated by NVCs. Refining the framework to explicitly incorporate composition-meteorology interactions is therefore essential for accurately predicting aerosol acidity in coastal regions subject to extreme weather events.

3.3 Atmospheric implications. In densely populated continental regions, where anthropogenic emissions and atmospheric ammonia concentrations are high, aerosol pH is likely controlled by the NH_4^+/NH_3 buffering pair and can therefore be reasonably approximated on the basis of aerosol mass concentration and liquid water content. This provides an opportunity to reconstruct long-term trends and large-scale spatial distributions of aerosol pH, and implies that emission reductions targeting ammonia and sulfate can exert direct and predictable influences on aerosol acidity.

In coastal regions, however, whether ammonia serves as the dominant buffering pair is strongly influenced by seasonality and meteorological conditions. Our field observations directly captured two contrasting situations: a non-typhoon period, in which ammonia acted as the dominant buffering pair, and a typhoon period, during which NVCs played a more important role. In the former case, aerosol pH can be reliably predicted using only aerosol mass concentration and AWC, whereas in the latter case, more detailed chemical composition information is required for accurate prediction. Acidity regulation in coastal area is inherently more variable than in continental settings, with rapid transitions between meteorological and compositional control. Such variability complicates the prediction of secondary aerosol formation and the assessment of pH-dependent processes (e.g., metal solubility and heterogeneous chemistry). Our results therefore underscore the need for improved representation of composition-meteorology interactions in chemical transport models and highlight the need for targeted observations during extreme weather events to constrain acidity regulation in coastal atmospheres.

https://doi.org/10.5194/egusphere-2025-4757
Preprint. Discussion started: 6 October 2025

Data availability. Data used to produce the plots within this work are available in Zenodo (https://zenodo.org/records/17207845).

Author contributions. JZ and XY designed the study. JZ and YZ analyzed the data. JZ wrote the manuscript. All co-authors contributed to discussions and suggestions in finalizing the manuscript.

Competing interests. The contact author has declared that none of the authors has any competing interests.

Acknowledgments. The authors would like to thank the Shenzhen National Climate Observatory for providing the observation platform for this study.

Financial support. This work was supported by the National Natural Science Foundation of China (42305108, 42530609), the Guangdong Basic and Applied Research Foundation (2025A1515011148), the Guangdong Provincial Observation and Research Station for Coastal Atmosphere and Climate of the Greater Bay Area (2021B1212050024), the Shenzhen Science and Technology Program (KQTD20210811090048025, KCXFZ20230731093601003), and the Ministry of Science and Technology of the People's Republic of China (2023YFE0112901).

https://doi.org/10.5194/egusphere-2025-4757
Preprint. Discussion started: 6 October 2025

References:

Amdur, M. O., Bayles, J., Ugro, V., and Underhill, D. W.: Comparative irritant potency of sulfate salts, Environ. Res., 16, 1-8, 10.1016/0013-9351(78)90135-4, 1978.

Battaglia, M. A., Douglas, S., and Hennigan, C. J.: Effect of the Urban Heat Island on Aerosol pH, Environ. Sci. Technol., 51, 13095-13103, 10.1021/acs.est.7b02786, 2017.

Battaglia, M. A., Weber, R. J., Nenes, A., and Hennigan, C. J.: Effects of water-soluble organic carbon on aerosol pH, Atmos. Chem. Phys., 19, 14607-14620, 10.5194/acp-19-14607-2019, 2019.

Bian, Y. X., Zhao, C. S., Ma, N., Chen, J., and Xu, W. Y.: A study of aerosol liquid water content based on hygroscopicity measurements at high relative humidity in the North China Plain, Atmos. Chem. Phys., 14, 6417-6426, 10.5194/acp-14-6417-2014, 2014.

Boyer, H. C., Gorkowski, K., and Sullivan, R. C.: In Situ pH Measurements of Individual Levitated Microdroplets Using Aerosol Optical Tweezers, Anal. Chem., 92, 1089-1096, 10.1021/acs.analchem.9b04152, 2020.

Cai, B. H., Wang, Y. X., Yang, X., Li, Y. C., Zhai, J. H., Zeng, Y. L., Ye, J. H., Zhu, L., Fu, T. M., and Zhang, Q.: Rapid aqueous-phase dark reaction of phenols with nitrosonium ions: Novel mechanism for atmospheric nitrosation and nitration at low pH, PNAS Nexus, 3, 10.1093/pnasnexus/pgae385, 2024.

Chen, Z., Liu, P., Su, H., and Zhang, Y. H.: Displacement of Strong Acids or Bases by Weak Acids or Bases in Aerosols: Thermodynamics and Kinetics, Environ. Sci. Technol., 10.1021/acs.est.2c03719, 2022.

Clegg, S. L., Pitzer, K. S., and Brimblecombe, P.: Thermodynamics of multicomponent, miscible, ionic-solutions. 2. Mixtures including unsymmetrical electrolytes, J. Phys. Chem., 96, 9470-9479, 10.1021/j100202a074, 1992.

Craig, R. L., Peterson, P. K., Nandy, L., Lei, Z., Hossain, M. A., Camarena, S., Dodson, R. A., Cook, R. D., Dutcher, C. S., and Ault, A. P.: Direct Determination of Aerosol pH: Size-Resolved Measurements of Submicrometer and Supermicrometer Aqueous Particles, Anal. Chem., 90, 11232-11239, 10.1021/acs.analchem.8b00586, 2018.

Cui, X. Y., Tang, M. J., Wang, M. J., and Zhu, T.: Water as a probe for pH measurement in individual particles using micro-Raman spectroscopy, Anal. Chim. Acta, 1186, 10.1016/j.aca.2021.339089, 2021.

Ding, J., Zhao, P. S., Su, J., Dong, Q., Du, X., and Zhang, Y. F.: Aerosol pH and its driving factors in Beijing, Atmos. Chem. Phys., 19, 7939-7954, 10.5194/acp-19-7939-2019, 2019.

Fang, T., Guo, H. Y., Zeng, L. H., Verma, V., Nenes, A., and Weber, R. J.: Highly Acidic Ambient

https://doi.org/10.5194/egusphere-2025-4757
Preprint. Discussion started: 6 October 2025

Particles, Soluble Metals, and Oxidative Potential: A Link between Sulfate and Aerosol Toxicity, Environ. Sci. Technol., 51, 2611-2620, 10.1021/acs.est.6b06151, 2017.

Gao, J., Wei, Y. T., Wang, H. Q., Song, S. J., Xu, H., Feng, Y. C., Shi, G. L., and Russell, A. G.: Multiphase Buffering: A Mechanistic Regulator of Aerosol Sulfate Formation and Its Dominant Pathways, Environ. Sci. Technol., 59, 8073-8084, 10.1021/acs.est.4c13744, 2025.

Guo, H., Xu, L., Bougiatioti, A., Cerully, K. M., Capps, S. L., Hite, J. R., Carlton, A. G., Lee, S. H., Bergin, M. H., Ng, N. L., Nenes, A., and Weber, R. J.: Fine-particle water and pH in the southeastern United States, Atmos. Chem. Phys., 15, 5211-5228, 10.5194/acp-15-5211-2015, 2015.

Guo, H. Y., Otjes, R., Schlag, P., Kiendler-Scharr, A., Nenes, A., and Weber, R. J.: Effectiveness of ammonia reduction on control of fine particle nitrate, Atmos. Chem. Phys., 18, 12241-12256, 10.5194/acp-18-12241-2018, 2018.

Hennigan, C. J., Izumi, J., Sullivan, A. P., Weber, R. J., and Nenes, A.: A critical evaluation of proxy methods used to estimate the acidity of atmospheric particles, Atmos. Chem. Phys., 15, 2775-2790, 10.5194/acp-15-2775-2015, 2015.

Jacobson, M. Z., Tabazadeh, A., and Turco, R. P.: Simulating equilibrium within aerosols and nonequilibrium between gases and aerosols, J. Geophys. Res. Atmos., 101, 9079-9091, 10.1029/96jd00348, 1996.

Karydis, V. A., Tsimpidi, A. P., Pozzer, A., and Lelieveld, J.: How alkaline compounds control atmospheric aerosol particle acidity, Atmos. Chem. Phys., 21, 14983-15001, 10.5194/acp-21-14983-2021, 2021.

Li, W. H., and Kuwata, M.: Detecting pH of Sub-Micrometer Aerosol Particles Using Fluorescent Probes, Environ. Sci. Technol., 57, 8701-8707, 10.1021/acs.est.3c01517, 2023.

Longo, A. F., Feng, Y., Lai, B., Landing, W. M., Shelley, R. U., Nenes, A., Mihalopoulos, N., Violaki, K., and Ingall, E. D.: Influence of Atmospheric Processes on the Solubility and Composition of Iron in Saharan Dust, Environ. Sci. Technol., 50, 6912-6920, 10.1021/acs.est.6b02605, 2016.

Metzger, S., Mihalopoulos, N., and Lelieveld, J.: Importance of mineral cations and organics in gas-aerosol partitioning of reactive nitrogen compounds: case study based on MINOS results, Atmos. Chem. Phys., 6, 2549-2567, 10.5194/acp-6-2549-2006, 2006.

Nenes, A., Pandis, S. N., and Pilinis, C.: ISORROPIA: A new thermodynamic equilibrium model for multiphase multicomponent inorganic aerosols, Aquat. Geochem., 4, 123-152, 10.1023/a:1009604003981, 1998.

Nenes, A., Pandis, S. N., and Pilinis, C.: Continued development and testing of a new thermodynamic aerosol module for urban and regional air quality models, Atmos. Environ., 33,

https://doi.org/10.5194/egusphere-2025-4757
Preprint. Discussion started: 6 October 2025

1553-1560, 10.1016/s1352-2310(98)00352-5, 1999.

Pathak, R. K., Yao, X. H., and Chan, C. K.: Sampling artifacts of acidity and ionic species in PM2.5, Environ. Sci. Technol., 38, 254-259, 10.1021/es0342244, 2004.

Pilinis, C., and Seinfeld, J. H.: Continued development of a general equilibrium-model for inorganic multicomponent atmospheric aerosols, Atmos. Environ., 21, 2453-2466, 10.1016/0004-6981(87)90380-5, 1987.

Pye, H. O. T., Zuend, A., Fry, J. L., Isaacman-VanWertz, G., Capps, S. L., Appel, K. W., Foroutan, H., Xu, L., Ng, N. L., and Goldstein, A. H.: Coupling of organic and inorganic aerosol systems and the effect on gas-particle partitioning in the southeastern US, Atmos. Chem. Phys., 18, 357-370, 10.5194/acp-18-357-2018, 2018.

Pye, H. O. T., Nenes, A., Alexander, B., Ault, A. P., Barth, M. C., Clegg, S. L., Collett, J. L., Fahey, K. M., Hennigan, C. J., Herrmann, H., Kanakidou, M., Kelly, J. T., Ku, I. T., McNeill, V. F., Riemer, N., Schaefer, T., Shi, G. L., Tilgner, A., Walker, J. T., Wang, T., Weber, R., Xing, J., Zaveri, R. A., and Zuend, A.: The acidity of atmospheric particles and clouds, Atmos. Chem. Phys., 20, 4809-4888, 10.5194/acp-20-4809-2020, 2020.

Saxena, P., Hudischewskyj, A. B., Seigneur, C., and Seinfeld, J. H.: A comparative-study of equilibrium approaches to the chemical characterization of secondary aerosols, Atmos. Environ., 20, 1471-1483, 10.1016/0004-6981(86)90019-3, 1986.

Song, S. J., Gao, M., Xu, W. Q., Shao, J. Y., Shi, G. L., Wang, S. X., Wang, Y. X., Sun, Y. L., and McElroy, M. B.: Fine-particle pH for Beijing winter haze as inferred from different thermodynamic equilibrium models, Atmos. Chem. Phys., 18, 7423-7438, 10.5194/acp-18-7423-2018, 2018.

Song, X. W., Wu, D., Chen, X., Ma, Z. Z., Li, Q., and Chen, J. M.: Toxic Potencies of Particulate Matter from Typical Industrial Plants Mediated with Acidity via Metal Dissolution, Environ. Sci. Technol., 58, 6736-6743, 10.1021/acs.est.4c00929, 2024.

Surratt, J. D., Lewandowski, M., Offenberg, J. H., Jaoui, M., Kleindienst, T. E., Edney, E. O., and Seinfeld, J. H.: Effect of acidity on secondary organic aerosol formation from isoprene, Environ. Sci. Technol., 41, 5363-5369, 10.1021/es0704176, 2007.

Tao, Y., and Murphy, J. G.: The sensitivity of PM2.5 acidity to meteorological parameters and chemical composition changes: 10-year records from six Canadian monitoring sites, Atmos. Chem. Phys., 19, 9309-9320, 10.5194/acp-19-9309-2019, 2019.

Tao, Y., and Murphy, J. G.: Simple Framework to Quantify the Contributions from Different Factors Influencing Aerosol pH Based on NHx Phase-Partitioning Equilibrium, Environ. Sci. Technol., 55, 10310-10319, 10.1021/acs.est.1c03103, 2021.

Tilgner, A., Schaefer, T., Alexander, B., Barth, M., Collett, J. L., Fahey, K. M., Nenes, A., Pye, H.

https://doi.org/10.5194/egusphere-2025-4757
Preprint. Discussion started: 6 October 2025

456 O. T., Herrmann, H., and McNeill, V. F.: Acidity and the multiphase chemistry of atmospheric
457 aqueous particles and clouds, Atmos. Chem. Phys., 21, 13483-13536, 10.5194/acp-21-13483-
458 2021, 2021.

459 Turnock, S. T., Mann, G. W., Woodhouse, M. T., Dalvi, M., O'Connor, F. M., Carslaw, K. S., and
460 Spracklen, D. V.: The Impact of Changes in Cloud Water pH on Aerosol Radiative Forcing,
461 Geophys. Res. Lett., 46, 4039-4048, 10.1029/2019gl082067, 2019.

462 Wang, G. C., Tao, Y., Chen, J., Liu, C. F., Qin, X. F., Li, H., Yun, L., Zhang, M. D., Zheng, H. T.,
463 Gui, H. Q., Liu, J. G., Huo, J. T., Fu, Q. Y., Deng, C. R., and Huang, K.: Quantitative
464 Decomposition of Influencing Factors to Aerosol pH Variation over the Coasts of the South
465 China Sea, East China Sea, and Bohai Sea, Environmental Science & Technology Letters, 9,
466 815-821, 10.1021/acs.estlett.2c00527, 2022.

467 Wexler, A. S., and Seinfeld, J. H.: Second-generation inorganic aerosol model, Atmos. Environ.
468 Part A. General Topics, 25, 2731-2748, https://doi.org/10.1016/0960-1686(91)90203-J, 1991.

469 Wexler, A. S., and Clegg, S. L.: Atmospheric aerosol models for systems including the ions H+,
470 NH4+, Na+, SO42-, NO3-,Cl-, Br-, and H2O, J. Geophys. Res. Atmos., 107,
471 10.1029/2001jd000451, 2002.

472 Xie, Y. N., Wang, G. H., Wang, X. P., Chen, J. M., Chen, Y. B., Tang, G. Q., Wang, L. L., Ge, S.
473 S., Xue, G. Y., Wang, Y. S., and Gao, J.: Nitrate-dominated PM2.5 and elevation of particle pH
474 observed in urban Beijing during the winter of 2017, Atmos. Chem. Phys., 20, 5019-5033,
475 10.5194/acp-20-5019-2020, 2020.

476 Xu, Y., Miyazaki, Y., Tachibana, E., Sato, K., Ramasamy, S., Mochizuki, T., Sadanaga, Y.,
477 Nakashima, Y., Sakamoto, Y., Matsuda, K., and Kajii, Y.: Aerosol Liquid Water Promotes the
478 Formation of Water-Soluble Organic Nitrogen in Submicrometer Aerosols in a Suburban Forest,
479 Environ. Sci. Technol., 54, 1406-1414, 10.1021/acs.est.9b05849, 2020.

480 Zhai, J. H., Zhang, Y., Liu, P. F., Zhang, Y. J., Zhang, A. T., Zeng, Y. L., Cai, B. H., Zhang, J. Y.,
481 Xing, C. B., Yang, H. L., Wang, X. F., Ye, J. H., Wang, C., Fu, T. M., Zhu, L., Shen, H. Z., Tao,
482 S., and Yang, X.: Source-dependent optical properties and molecular characteristics of
483 atmospheric brown carbon, Atmos. Chem. Phys., 25, 7959-7972, 10.5194/acp-25-7959-2025,
484 2025.

485 Zhang, A. T., Zeng, Y. L., Yang, X., Zhai, J. H., Wang, Y. X., Xing, C. B., Cai, B. H., Shi, S., Zhang,
486 Y. J., Shen, Z. X., Fu, T. M., Zhu, L., Shen, H. Z., Ye, J. H., and Wang, C.: Organic Matrix Effect
487 on the Molecular Light Absorption of Brown Carbon, Geophys. Res. Lett., 50,
488 10.1029/2023gl106541, 2023.

489 Zhang, B. Q., Shen, H. Z., Liu, P. F., Guo, H. Y., Hu, Y. T., Chen, Y. L., Xie, S. D., Xi, Z. Y.,
490 Skipper, T. N., and Russell, A. G.: Significant contrasts in aerosol acidity between China and
491 the United States, Atmos. Chem. Phys., 21, 8341-8356, 10.5194/acp-21-8341-2021, 2021.

https://doi.org/10.5194/egusphere-2025-4757
Preprint. Discussion started: 6 October 2025

492 Zheng, G. J., Su, H., Wang, S. W., Andreae, M. O., Pöschl, U., and Cheng, Y. F.: Multiphase buffer
493 theory explains contrasts in atmospheric aerosol acidity, Science, 369, 1374-+,
494 10.1126/science.aba3719, 2020.

495 Zheng, G. J., Su, H., and Cheng, Y. F.: Revisiting the Key Driving Processes of the Decadal Trend
496 of Aerosol Acidity in the U.S, ACS Environ. Au, 2, 346-353, 10.1021/acsenvironau.1c00055,
497 2022.

498 Zhou, M., Zheng, G. J., Wang, H. L., Qiao, L. P., Zhu, S. H., Huang, D. D., An, J. Y., Lou, S. R.,
499 Tao, S. K., Wang, Q., Yan, R. S., Ma, Y. G., Chen, C. H., Cheng, Y. F., Su, H., and Huang, C.:
500 Long-term trends and drivers of aerosol pH in eastern China, Atmos. Chem. Phys., 22, 13833-
501 13844, 10.5194/acp-22-13833-2022, 2022.